Monthly Notices
of the
ROYAL ASTRONOMICAL SOCIETY

MNRAS **501,** 911–915 (2021)
Advance Access publication 2020 December 2

doi:10.1093/mnras/staa3732

The Y dwarf population with *HST*: unlocking the secrets of our coolest neighbours – I. Overview and first astrometric results

C. Fontanive [1]★, L. R. Bedin [2] and D. C. Bardalez Gagliuffi[3]

[1] *Center for Space and Habitability, University of Bern, Gesellschaftsstrasse 6, CH-3012 Bern, Switzerland*
[2] *INAF – Osservatorio Astronomico di Padova, Vicolo dell'Osservatorio 5, I-35122 Padova, Italy*
[3] *American Museum of Natural History, 200 Central Park West, New York, NY 10024, USA*

Accepted 2020 November 27. Received 2020 November 13; in original form 2020 October 5

ABSTRACT

In this paper, we present our project that aims at determining accurate distances and proper motions for the Y brown dwarf population using the *Hubble Space Telescope*. We validate the program with our first results, using a single new epoch of observations of the Y0pec dwarf WISE J163940.83−684738.6. These new data allowed us to refine its proper motion and improve the accuracy of its parallax by a factor of three compared to previous determinations, now constrained to $\varpi = 211.11 \pm 0.56$ mas. This newly derived absolute parallax corresponds to a distance of 4.737 ± 0.013 pc, an exquisite and unprecedented precision for faint ultracool Y dwarfs.

Key words: brown dwarfs – stars: individual: WISE J163940.83−684738.6.

1 INTRODUCTION

The new Y spectral sequence (Cushing et al. 2011), classifying objects with effective temperatures <500 K, is filling a crucial gap in mass and temperature between brown dwarfs and Jupiter, offering ideal proxies to study planet-like atmospheres (Skemer et al. 2016). However, fewer than ∼30 isolated Y dwarfs have been confirmed so far,[1] and large disparities are seen within the uneven sets of limited data available, due to the challenges associated with astrometric and spectrophotometric observations for such intrinsically faint objects. The lack of reliable distance estimates to calibrate these systems is a key factor in our poor understanding of their physical and atmospheric properties. Indeed, accurate distances are vital for confident interpretations of measured quantities and assessments of inherent properties, which are thus indispensable to characterize these pivotal giant planet analogues.

Dedicated programs aim at deriving trigonometric parallaxes for nearby brown dwarfs from the ground (Tinney et al. 2014; Liu, Dupuy & Allers 2016; Best et al. 2020) and from space (Dupuy & Kraus 2013; Martin et al. 2018; Kirkpatrick et al. 2019). However, the typical precision reached in these observationally expensive campaigns (a few to tens of mas) results in substantial uncertainties in the underlying distances, and significant disagreements are observed between programs for the faintest targets (e.g. Beichman et al. 2014).

We present here the first results of our new *Hubble Space Telescope* (*HST*) project (GO 16229, PI: Fontanive), designed to measure the most precise parallaxes and proper motions to date for the majority of the ultracool Y dwarf population. *HST* provides a unique platform to obtain precise astrometric parameters for Y dwarfs, with a remarkable astrometric precision and unmatched capabilities at near-infrared wavelengths for observations of such cold objects. By exploiting the *Gaia* Data Release 2 (DR2; Gaia Collaboration 2016, 2018) astrometric solutions for bright stars in *HST* field of views, the exquisite astrometric precision of *HST* can be translated into an absolute reference frame with an equally exquisite astrometric accuracy. In particular, the combination of *HST* and *Gaia* DR2 in this way can enable the derivation of astrometric parameters with *Gaia*-level precisions for sources like Y dwarfs that are certainly too dim for *Gaia*. In Bedin & Fontanive (2018, 2020), we demonstrated that such an approach can achieve uncertainties of less than 2 mas on parallaxes and at the ∼0.3-mas level on proper motions, with a minimal three epochs of *HST* observations acquired over ∼half a decade.

With this program, we will obtain the final epochs of observations required to implement this procedure for 19 Y dwarfs. Combined to archival data, these observations will allow us to derive reliable and uniform astrometric parameters for these objects, constraining distances and kinematics for the vast majority of the existing population of Y dwarfs. In this paper, we use new *HST* data of the Y0pec dwarf WISE J163940.83−684738.6 to refine its parallax and proper motion and validate our approach. We introduce the target in Section 2, and describe the observations in Section 3. Section 4 presents our analysis, with an overview of our astrometric method from Bedin & Fontanive (2018, 2020) and the new results for the studied target. Our conclusions and outlook for the project are summarized in Section 5.

2 W1639−6847

WISE J163940.83−684738.6 (hereafter W1639−6847) is a nearby Y0pec ultracool brown dwarf, first discovered in Tinney et al. (2012) and subsequently classified by Tinney et al. (2014) and Schneider et al. (2015). Model-derived physical parameters for this brown dwarf are highly uncertain and in some cases rather unrealistic (Leggett

★ E-mail: clemence.fontanive@csh.unibe.ch
[1] https://sites.google.com/view/ydwarfcompendium/home

et al. 2017; Zalesky et al. 2019). This is likely due to a combination of the deviant spectrophotometric features of this outlier brown dwarf, and the somewhat unreliable distance to the object available at the time of these studies (see Bedin & Fontanive 2020 for details).

We used this target in Bedin & Fontanive (2020) to refine our *HST*-based astrometric method (see Section 4.3) first presented in Bedin & Fontanive (2018). W1639−6847 was a prime target for our approach, with three epochs of *HST* observations taken between 2013 and 2019, and several independent – but rather inconsistent – measurements of its parallax and proper motion available in the literature (Tinney et al. 2012, 2014; Pinfield et al. 2014; Martin et al. 2018; Kirkpatrick et al. 2019).

By anchoring these three epochs of *HST* data acquired over ∼6 yr to the *Gaia* DR2 reference frame, we were able to constrain its astrometric parameters to unprecedented *Gaia*-like precisions (Bedin & Fontanive 2020). The achieved precisions of ∼2 mas on the parallax and at the sub-mas level on the proper motion already represented considerable improvements over previous estimates. None the less, this parallax estimate for W1639−6847 relied entirely on the data set with the lowest astrometric precision among the *HST* epochs available at the time, which also did not provide an optimal coverage of the yearly parallax ellipse, leaving room for improvement on the astrometric parameters of this benchmark brown dwarf.

3 OBSERVATIONS

Previous *HST* data sets for W1639−6847 consist of three separate epochs with a total of 18 infrared (IR) images, described in Bedin & Fontanive (2020). We recently acquired new *HST* observations of this target as part of our dedicated program, GO 16229 (PI: Fontanive), with data taken on 2020 September 2.

The new data consist of a single epoch made of eight exposures in the *F*160*W* filter, collected over one full *HST* orbit with the (IR) channel of the Wide Field Camera 3 (WFC3) instrument. During the orbit, a large eight-point dither pattern was chosen, with a deep image obtained at each dithered position. The first four exposures were of duration 302.938 s each, followed by four exposures of 327.939 s. All images were acquired in MULTIACCUM mode with SAMP-SEQ=SPARS25, using NSAMP=13 samples for the former set of exposures and NSAMP=14 for the latter, for a total exposure time of 2523.508 s in the *F*160*W* band. The observations were planned so as to keep the target at the centre of the field of view (FoV) instead of remapping the FoV of previous data sets, a choice driven by the method described in Bedin & Fontanive (2018, 2020), which relies entirely on *Gaia* DR2 stars.

A total of 26 individual images (18 + 8) are therefore employed for the analysis described in the following section.

4 ANALYSIS

The data reduction and analyses of this work follow the exact steps presented in Bedin & Fontanive (2018, 2020), adding the data from the newest epoch of the science target, reduced in the same way as previous data sets. We briefly summarize these methods below but refer the reader to those original works for detailed descriptions of the procedures and extensive discussions.

4.1 Data reduction

Positions and magnitudes of detected sources were extracted in every WFC3/IR flat-fielded image from the newest *HST* data set, using the publicly available software developed by J. Anderson (Anderson & King 2006). Measured positions in raw pixel coordinates were then corrected for the distortion of the camera.[2] For all sources sufficiently bright to be in the *Gaia* DR2 catalogue with full five-parameter astrometric solutions, the positions of detected stars were then placed into the ICRS frame, transforming their *Gaia* positions to the specific epoch of the *HST* observations using the sources' parallaxes and proper motions, thus linking the *HST* reference frame to the *Gaia* DR2 system. The procedure involves going back and forth to the tangential plane, using the methods and equations detailed in section 3 of Bedin & Fontanive (2018).

The same tasks were already performed for the previous observational data sets in Bedin & Fontanive (2020), reregistering each frame on to the observational plane at epoch 2013.12, and the new data were similarly linked to the same reference system. This provides us with a common reference frame for all images from the various available epochs, defined by *Gaia* DR2 anchor sources that can be repositioned to the relevant epochs from their respective *Gaia* DR2 astrometric solutions. This allows us to transform the positions of every detected source to the absolute ICRS reference frame for every image and epoch, including sources much dimmer than those detectable by *Gaia*, such as our extremely faint Y dwarf science target.

Table 1. Absolute astrometric parameters of W1639−6847 in the ICRS reference frame. Positions are given at 2000.0 and 2015.5. Note the larger errors for epoch 2000.0, as result of a large extrapolation to this epoch.

Parameter	Value	Uncertainty
$\alpha_{2000.0}$ ($^{h\,m\,s}$)	16:39:39.730	± 12 mas
$\delta_{2000.0}$ ($^{\circ}\,'\,''$)	−68:47:06.693	± 4 mas
$\alpha_{2000.0}$ (deg)	249.915540	± 12 mas
$\delta_{2000.0}$ (deg)	−68.785192	± 4 mas
$\alpha_{2015.5}$ (deg)	249.9224084	± 4.5 mas
$\delta_{2015.5}$ (deg)	−68.79857156	± 0.8 mas
$\mu_{\alpha\cos\delta}$ (mas yr^{-1})	+576.94	± 0.22
μ_{δ} (mas yr^{-1})	−3108.48	± 0.21
ϖ (mas)	211.11	± 0.56 (±0.05)[a]

Note. [a]Systematic uncertainties inherent to *Gaia* DR2 parallaxes.

4.2 Stack images

From these coordinate transformations into the common reference frame, we created stacked images for the latest observations of W1639−6847, complementing those from Bedin & Fontanive (2020) for the previous epochs and available online. We provide the newest stacks in the *F*160*W* filter as supplementary electronic material, saved in `fits` format, with the absolute astrometric solution provided in the header World Coordinate System keyword (see Bedin & Fontanive 2018, 2020 for additional details about the stacked images).

4.3 Determination of the astrometric parameters

The 26 individual *HST* images available for W1639−6847 each yield a 2D positional measurement of the brown dwarf. This provides us

[2]Jay Anderson made publicly available the WFC3/IR distortion solution and the point spread functions (PSFs) he derived in Anderson (2016), also providing softwares to use them. This material can be found at https://www.stsci.edu/~jayander/WFC3/, where the subdirectory `WFC3_GC/` contains the distortion solution, and `WFC3_PSFs` the PSFs for various filters.

Table 2. Comparison of our new absolute astrometric parameters for W1639−6847 with the most precise estimates in the literature.

Work #. Authors (date)	$\mu_{\alpha^*} \pm \sigma\mu_{\alpha^*}$ (mas yr^{-1})	$\mu_\delta \pm \sigma\mu_\delta$ (mas yr^{-1})	$\varpi \pm \sigma_\varpi$ (mas)	d (pc)	Source facilities
1. Kirkpatrick et al. (2019)	582.0 ± 1.5	−3099.8 ± 1.5	211.9 ± 2.7	4.72 ± 0.06	*Spitzer* + *Gaia* DR1
2. Bedin & Fontanive (2020)	577.21 ± 0.24	−3108.39 ± 0.27	210.35 ± 1.82	4.75 ± 0.05	*HST* + *Gaia* DR2
3. This work	576.94 ± 0.22	−3108.48 ± 0.21	211.11 ± 0.56	4.737 ± 0.013	*HST* + *Gaia* DR2

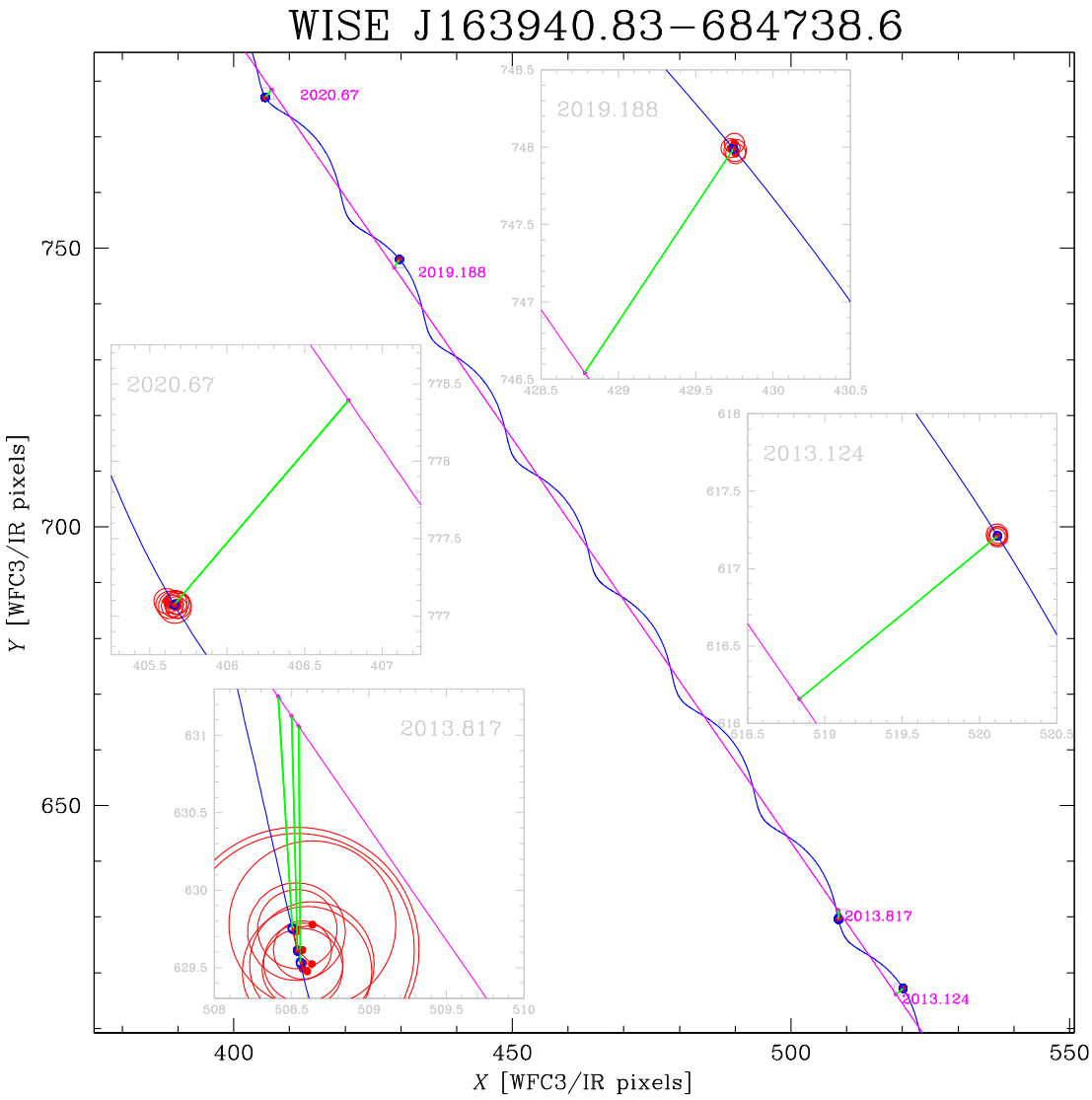

Figure 1. Comparison of our astrometric solution (blue line) with the individual observed data points (red bullets) for W1639−6847 in the distortion-corrected observational plane at epoch 2013.12. The four major epochs are labelled, with insets labelled accordingly showing a more meaningful zoom-in of the data points. The sizes of the red circles indicate the quality-fit parameter (Anderson et al. 2008) for each data point, with smaller radii for better measurements. To better highlight the parallax component of the motion, a magenta line marks the motion of an object with the same proper motion but placed at infinite distance (i.e. with zero parallax). Green lines show the parallax contributions at each epoch, and red segments connect the individual data points with their expected positions (blue bullets on the blue line) according to the best fit.

with a total of 52 individual data points to infer five astrometric parameters: the position (α, δ), proper motion ($\mu_{\alpha\cos\delta}$, μ_δ), and absolute parallax (ϖ). Following the methods described in Bedin & Fontanive (2018, 2020), we used the Naval Observatory Vector Astrometry Software (NOVAS) tool from the U.S. Naval Observatory (Kaplan et al. 2011) to compute time-dependent positions for stars based on ICRS coordinates, proper motions, and parallaxes. We then used a Levenberg–Marquardt algorithm (Moré, Garbow & Hillstrom 1980) to find the minimization of the five parameters for W1639−6847.

Our results are presented in Table 1, and compared in Table 2 to our previous determinations and the *Spitzer*-derived astrometry from Kirkpatrick et al. (2019; see Bedin & Fontanive 2020 for a complete compilation of astrometric measurements for W1639−6847 in the literature). The 0.05 mas added to the error budget of ϖ is for the systematic uncertainties inherent to *Gaia* DR2 parallaxes

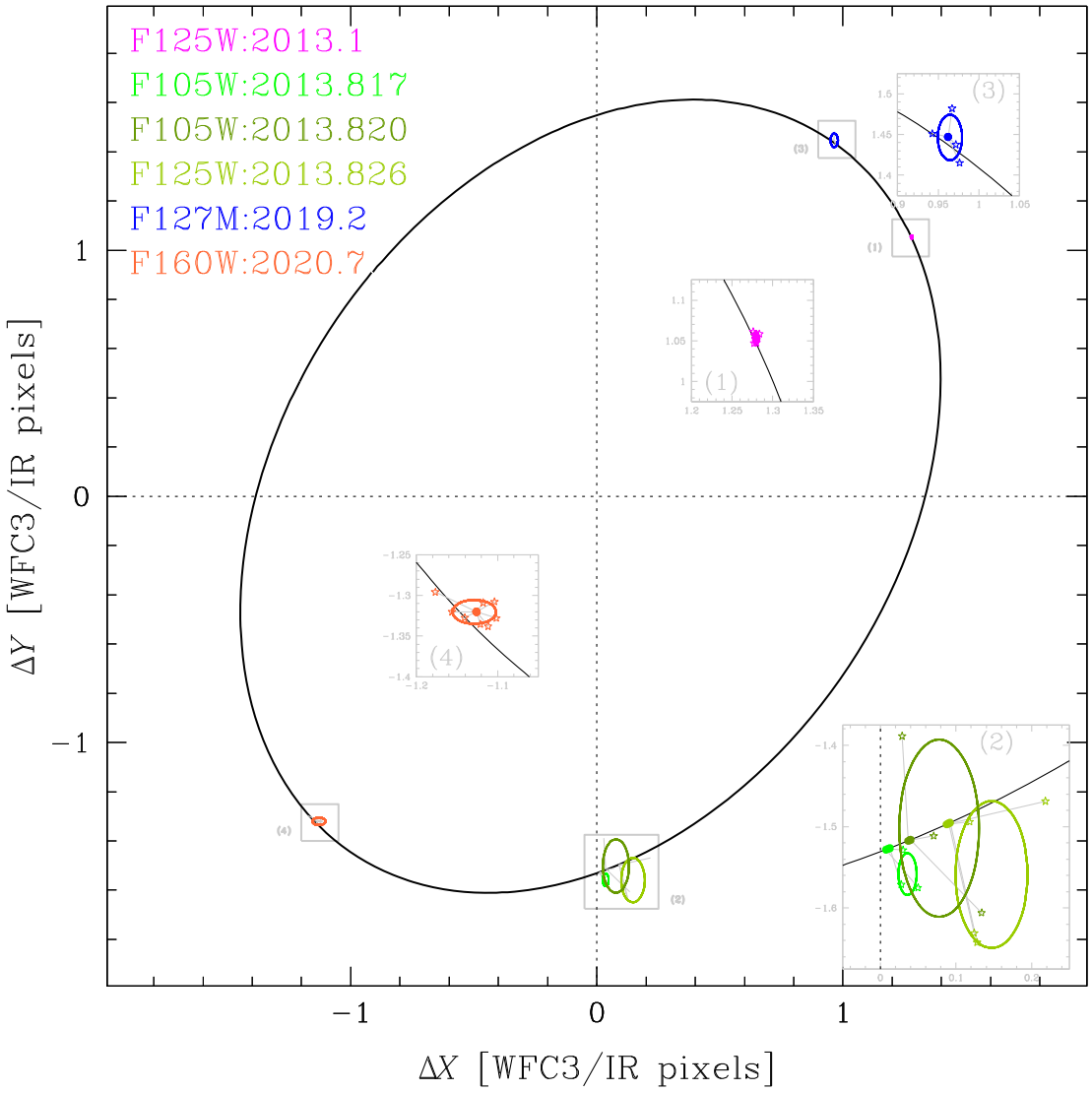

Figure 2. Our solution for the parallax ellipse in the distortion-corrected reference coordinate system at epoch 2013.12. Individual *HST* data points are indicated with star symbols, connected with small segments to their expected best-fitting positions. Smaller ellipses indicate the 1σ spread of individual data points within each epoch. Note how ellipses are significantly smaller for the first and the last two epochs (magenta, blue, and orange), compared to the 2013.8 subepochs (various shades of green). Insets in grey all have the same scale, and show zoom-in views around the locations marked by grey boxes.

(Lindegren et al. 2018), although inconsequential compared to the estimated parallax error. Fig. 1 shows our best-fitting solution for the proper motion and parallax of the Y dwarf, along with the *HST* measurements at each epoch. Fig. 2 displays the parallax ellipse of the target, subtracting the proper motion from the total displacement.

As discussed in Bedin & Fontanive (2020), the parallax estimate derived in that work for W1639−6847 relied entirely on the epoch with the lowest astrometric precision (degraded by a nearby star and anomalously high background level; epoch plotted in green in Fig. 2), thus requiring an additional epoch of observations to be further validated and refined. We demonstrate here that our new epoch, optimally timed to measure the maximum parallax elongation (orange epoch in Fig. 2), is sufficient to improve the accuracy of the parallax by a factor of more than 3 over our previous estimate. As expected, improvements on proper motions and positions are, instead, marginal, since these quantities were already well constrained by two epochs widely separated in time and with high astrometric accuracies taken at the same phase of the year (blue and magenta epochs).

We also tested the robustness of our astrometric solution by excluding the degraded epoch 2013.8 from our fit. The astrometric solution derived without this poorer data set is fully consistent with our main results within uncertainties (parallax within 0.02 mas, and even less significant disparities for proper motions and positions). This is not surprising given that data points are weighted with the quality-of-fit parameter (see Bedin & Fontanive 2018, 2020), and the data points from the 2013.8 epoch thus have the lowest weight. With a lower significance towards our coverage of the full parallax elongation, now optimized by the first and last two observational epochs, this intermediate data set has a negligible influence towards the final solution.

5 CONCLUSIONS AND OUTLOOK

With a new epoch of *HST* observations for W1639−6847 designed specifically to complement archival *HST* data, we were able to constrain its astrometric parameters to unparalleled accuracies for such a faint ultracool brown dwarf. In particular, we achieved a 0.56-mas uncertainty on the parallax, a three-fold improvement over our previous estimate without this newest epoch (Bedin & Fontanive 2020; see Table 2). This is also considerably better than the precisions of a few to tens of mas typically reached in distance measurements for nearby Y dwarfs (Beichman et al. 2014; Martin et al. 2018; Kirkpatrick et al. 2019). Such results are only possible thanks to the higher angular resolution of *HST*/WFC3 compared to *Spitzer*, and the approach of cross-registration with *Gaia* sources. Our derived parallax corresponds to a remarkably precise distance of 4.737 ± 0.013 pc, which will incontestably be vital to investigate the peculiar nature and distinct atmospheric features of W1639−6847.

These results confirm the power of the method from Bedin & Fontanive (2018, 2020) to obtain highly precise astrometric measurements for the very faintest astronomical objects, by linking *HST* data to the *Gaia* absolute reference frame, hence validating our program. This paper notably demonstrates the necessity of optimally timed observations to achieve the best possible results on parallaxes and proper motions. Our ongoing *HST* campaign will last about 2 yr and will provide the new epochs needed to derive similar astrometric solutions for a total of 19 Y dwarfs. With observations carefully and strategically planned based on existing *HST* epochs for each object, at times of year both maximizing the coverage of the parallax ellipse and affording the best insights into proper motions, we anticipate comparable results for all targets in our sample.

Robust and uniform parallax measurements for the major part of the Y population will be essential to enhance our heavily scattered understanding of their characteristics, and improve theoretical models that severely lack empirical validation at the coldest temperatures (Schneider et al. 2015). Precise distances are indeed required for the knowledge of absolute fluxes, and therefore to estimate bolometric luminosities and unbiased spectral energy distributions. Measuring these quantities for benchmark objects to the highest levels of confidence will hence provide rich sources of testable fingerprints for theoretical models. The precise parallaxes anticipated from our program will also allow for detailed analyses of well-calibrated colour–magnitude diagrams, allowing for key probes of secondary effects like gravity or metallicity on the complex appearances of Y dwarfs, as well as the recognition of unresolved binarity. Constraining the kinematics and fundamental properties of these objects will also be crucial in preparation of upcoming missions like *JWST*, which, combined with robust calibrations, will offer invaluable new glimpses into these puzzling planetary atmospheres.

ACKNOWLEDGEMENTS

We thank the anonymous referee for a thorough review of our work, a constructive discussion and useful comments. CF acknowledges financial support from the Center for Space and Habitability (CSH, Ub). LRB acknowledges support by MIUR under PRIN program #2017Z2HSMF. This work has been carried out within the framework of the NCCR PlanetS supported by the Swiss National Science Foundation. This work is based on observations with the NASA/ESA *HST*, obtained at the Space Telescope Science Institute, which is operated by AURA, Inc., under NASA contract NAS 5-26555. This work makes also use of results from the European Space Agency (ESA) space mission *Gaia*. *Gaia* data are being processed by the Gaia Data Processing and Analysis Consortium (DPAC). Funding for the DPAC is provided by national institutions, in particular the institutions participating in the Gaia MultiLateral Agreement (MLA). The *Gaia* mission website is https://www.cosmos.esa.int/gaia. The *Gaia* archive website is https://archives.esac.esa.int/gaia. This research has benefitted from the Y Dwarf Compendium maintained by Michael Cushing at https://sites.google.com/view/ydwarfcompendium/.

Based on observations with the NASA/ESA *Hubble Space Telescope*, obtained at the Space Telescope Science Institute, which is operated by AURA, Inc., under NASA contract NAS 5-26555.

6 DATA AVAILABILITY

The reduced stacked images from this work are provided as supplementary electronic material.

REFERENCES

Anderson J., 2016, Instrument Science Report WFC3, Empirical Models for the WFC3/IR PSF. STScI, Baltimore, MD
Anderson J., King I. R., 2006, Technical Report, PSFs, Photometry, and Astronomy for the ACS/WFC, STScI, Baltimore, MD
Anderson J. et al., 2008, AJ, 135, 2055
Bedin L. R., Fontanive C., 2018, MNRAS, 481, 5339
Bedin L. R., Fontanive C., 2020, MNRAS, 494, 2068
Beichman C., Gelino C. R., Kirkpatrick J. D., Cushing M. C., Dodson-Robinson S., Marley M. S., Morley C. V., Wright E. L., 2014, ApJ, 783, 68
Best W. M. J., Liu M. C., Magnier E. A., Dupuy T. J., 2020, AJ, 159, 257
Cushing M. C. et al., 2011, ApJ, 743, 50
Dupuy T. J., Kraus A. L., 2013, Science, 341, 1492
Gaia Collaboration, 2016, A&A, 595, A1
Gaia Collaboration, 2018, A&A, 616, A1
Kaplan G., Bartlett J., Monet A., Bangert J., Puatua W., 2011, User's Guide to NOVAS Version F3.1. USNO, Washington, DC
Kirkpatrick J. D. et al., 2019, ApJS, 240, 19
Leggett S. K., Tremblin P., Esplin T. L., Luhman K. L., Morley C. V., 2017, ApJ, 842, 118
Lindegren L. et al., 2018, A&A, 616, A2
Liu M. C., Dupuy T. J., Allers K. N., 2016, ApJ, 833, 96
Martin E. C. et al., 2018, ApJ, 867, 109
Moré J. J., Garbow B. S., Hillstrom K. E., 1980, Argonne National Laboratory Report ANL-80-74, User Guide for MINPACK-1. Argonne National Laboratory, Illinois
Pinfield D. J. et al., 2014, MNRAS, 437, 1009
Schneider A. C. et al., 2015, ApJ, 804, 92
Skemer A. J. et al., 2016, ApJ, 826, L17
Tinney C. G., Faherty J. K., Kirkpatrick J. D., Wright E. L., Gelino C. R., Cushing M. C., Griffith R. L., Salter G., 2012, ApJ, 759, 60
Tinney C. G., Faherty J. K., Kirkpatrick J. D., Cushing M., Morley C. V., Wright E. L., 2014, ApJ, 796, 39
Zalesky J. A., Line M. R., Schneider A. C., Patience J., 2019, ApJ, 877, 24

SUPPORTING INFORMATION

Supplementary data are available at *MNRAS* online.

2020.7-F160W.fits

Please note: Oxford University Press is not responsible for the content or functionality of any supporting materials supplied by the authors. Any queries (other than missing material) should be directed to the corresponding author for the article.

This paper has been typeset from a TEX/LATEX file prepared by the author.